

Prediction Method of Crack Sensitivity during DC Casting of Al-Mn and Al-Mg Series Aluminum Alloys

Makoto Morishita¹, Mitsuhiro Abe¹ and Makoto Yoshida²

¹ Material & Process Research Section, Aluminum Sheets & Coil Research Department,
Moka Plant, Kobe Steel Ltd., 15 Kinugaoka, Moka-city, Tochigi 321-4367 Japan

² The Kagami Memorial Laboratory for Materials Science and Technology,
Waseda University, 2-8-26 Nishiwaseda Shinjuku-ku, Tokyo 169-0051 Japan

A new prediction method based on a relation between calculated solid fraction and temperature was developed concerning Al-Mn and Al-Mg series aluminum alloys. Two crack modes were considered in order to understand that the surface crack is located at ingot surface. The one is based on “the difference in strain between water chilling surface and mushy surface (crack mode Z)” and the other is on “the difference in strain rate between surface and just inner surface (crack mode Y)”. It was assumed that the high solid fraction region was from 0.75 to 0.95 (Region II) and two indexes were set up which are calculated from temperature difference (ΔT_{II}) and difference in a temperature drop per unit solid fraction ($\Delta R_{II}/\Delta T_{II}$) within the Region II. By using the both indexes, which were called “Brittle temperature range” and “Parameter of the strain rate difference” respectively, the crack sensitivities through DC casting experiments were suitably represented.

Keywords: DC casting, solidification cracking, alloy composition, solid fraction.

1. Introduction

In general, industrially used aluminum alloys contain various elements such as Fe, Si, Mn, Mg, Cu, Zn, and others as alloying components, and almost all of them involve eutectic reactions. An eutectic alloy containing these elements provides the solidus temperature more than 150K depending on alloys and the liquid phase remains even at low temperatures. This is why aluminum alloys are more sensitive to cast crack than pure aluminum.

Hitherto, as a crack sensitivity assessment method, an assessment process in that the wider the solidification temperature range, the more easily crack occurs has been popularly used, but this does not always comprehensively express the crack sensitivity in multi-component alloys. Consequently, to date, many researchers have reported on the crack mechanism and its sensitivity, such as a technique to calculate the relation between the values of ZST and ZDT and the solid fraction [1], thermal stress computation with high-temperature properties and mechanical characteristics incorporated [2], and others. However, no report has been so far made on the method for assessing crack sensitivity by alloying elements.

In this paper, a versatile and simple crack sensitivity assessment method, which was developed for the purpose of predicting surface crack sensitivity in vertical DC casting was evaluated experimentally. In addition, a surface crack generating model was devised, and consideration was made on the crack mode expressed by the crack sensitivity prediction indexes that can quantitatively assess surface crack.

2. Experimental method of crack sensitivity assessment

In order to examine crack sensitivity, a total of 10 alloys around on commonly-used Al-Mn and Al-Mg series, which had a wide range of chemical compositions shown in Table 1, were used.

In assessing the generation of cast crack, a vertical DC casting machine having a rectangular opening 400 mm wide and 150 mm thick was adopted. The length from the molten metal level to the mold exit was 65 mm and a float type controller was used for controlling the molten metal level.

The amount of cooling water was set constant at 100 L/min and the casting temperature was set constant to $983\pm 5K$. As soon as the molten metal reached the set molten metal surface level, casting was started at the casting rate of 60 mm/min to 100 mm/min. Because as the casting rate increased, the sensitivity to cast crack increased, the casting rate was designated as an operational factor of crack sensitivity in casting conditions. Presence of crack was determined visually or by the use of a dye penetrant.

3. Cast cracking test result

3.1 Assessment results of cast crack

Table 2 shows results of assessment of presence of cast crack and the solidification range (T_L-T_S) under the equilibrium. Cast crack was likely to be generated as the casting rate increased, and all cracks were observed on the surfaces.

This results indicate that it is not necessarily the case that alloys with wider solidification range are more sensitive to crack. This suggests that it is difficult to judge the sensitivity to crack by alloying components or solidification temperature range only.

3.2 Cast cracking form

Fig. 1 shows the examples of fracture surface obtained in the experiments. Reference symbols x , y , and z denote the width, thickness, and depth directions (casting directions), respectively. Cast crack was propagated from the surface to the thickness center position, and also propagated in the longitudinal direction to the end of castings. In order to identify the crack initiation point, SEM observation of fracture surface was made on the positions (A) through (D) as shown in Fig. 1.

As shown in Fig. 2, crack at the position (D) seems to have generated at higher temperature and it is suggested that at the position (D) fracture propagated earlier than at the positions (A), (B) or (C).

Based on the foregoing description, it can be concluded that the position (D) was a cast crack initiation point. Therefore further investigation was made on the DC cast crack with the solid-liquid coexisting zone on the ingot surface that corresponded to the location of the position (D).

Table 1 Chemical compositions of aluminum alloys used for this work. (mass%)

alloy	Si (mass%)	Fe (mass%)	Cu (mass%)	Mn (mass%)	Mg (mass%)
a	0.10	0.20	0.50	0.23	4.80
b	0.01	0.01	0.11	0.43	4.75
c	0.01	0.01	0.13	0.35	4.65
d	0.30	0.43	0.25	1.06	1.35
e	0.10	0.40	0.40	1.00	1.10
f	0.10	0.40	0.60	1.00	1.10
g	0.10	0.40	1.00	1.30	0.80
h	0.10	0.40	1.00	0.60	0.40
i	0.10	0.40	3.00	0.40	0.40
j	0.85	0.01	0.70	1.60	0.10

Table 2 Cracking results by DC casting experiment and calculated solidification range.

O: no cracking, X: cracking

alloy	Casting rate (mm/min)			Solidification range (K)
	60	80	100	
a	O	O	O	74.9
b	O	O	X	54.9
c	O	O	X	54.2
d	O	O	O	28.1
e	O	O	O	29.5
f	X	X	X	34.7
g	X	X	X	41.2
h	O	O	X	35.2
i	O	O	O	74.4
j	O	X	X	38.4

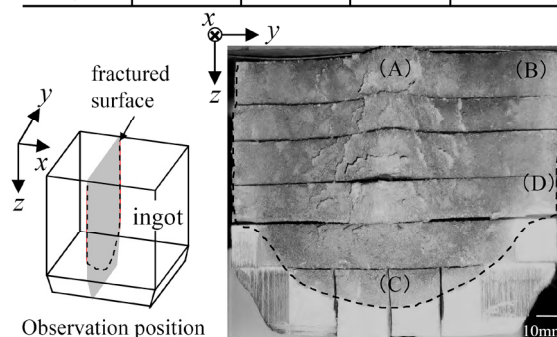


Fig. 1 Fractured surface of DC cast cracking.

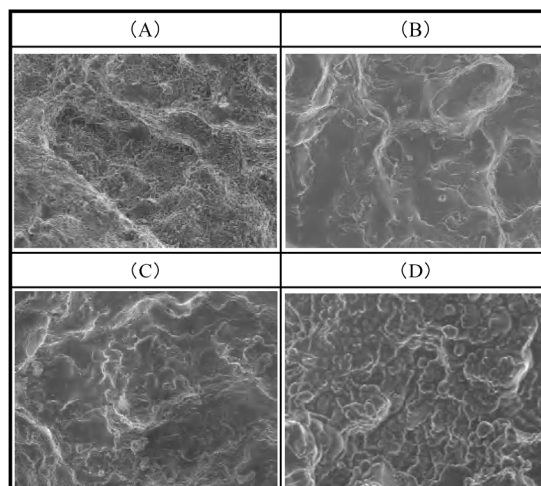


Fig. 2 SEM image of cast cracking fractured surface at (A)- (D) in Fig. 1. 50 μ m

4. Discussion on crack generation mode and crack sensitivity assessment indexes

4.1 Setting of the solid fraction region where solidification crack occurs

When a large amount of the liquid phase exists, the solid phase is scattered. Even if solid phases fracture, the solid phases are replenished with the melt and no crack occurs (Region I). On the other hand, in the case that a sufficient amount of solid phase exists, once solid phases fracture due to shrinkage strain of the solid phase, no melt is replenished and crack remains (Region II). It differs according to alloys, but in almost all alloy types, the ZDT is located in the range of 0.7 to 0.8 solid fraction [1,3]. Therefore, in the present paper, the solid fraction of 0.75 was set as the boundary between Region I and II, and it was assumed that solidification crack occurred in the solid fraction region with the solid fraction of exceeding 0.75.

According to high-temperature mechanical characteristics which were studied in the past, phenomena in which the critical strain (breaking strain) is excessively increased when the solid fraction exceeds about 0.95 [4]. In the present paper, it was assumed that in the region of the solid fraction exceeding 0.95, alloys provided ductility and no crack occurred (Region III).

Based on the foregoing description, it is the Region II that is the high solid fraction region in which crack remains due to temperature drop during solidification. In order to calculate the relation of the solid fraction to the temperature, thermo- dynamic software “Thermo-calc“ was applied.

4.2 Estimating the amount of strain and strain rate in the solid phase from the relation between temperature and solid fraction

As shown in the above- mentioned position (D), cast crack is generated from the solid-liquid coexisting zone on the ingot surface. With this temperature zone and the position set as a target, the authors assumed that crack tends to be generated in an area in the vicinity of the ingot surface that the amount of strain is large, and in the adjacent sections with a large difference in the strain rates. Then the authors considered that there were following two crack modes.

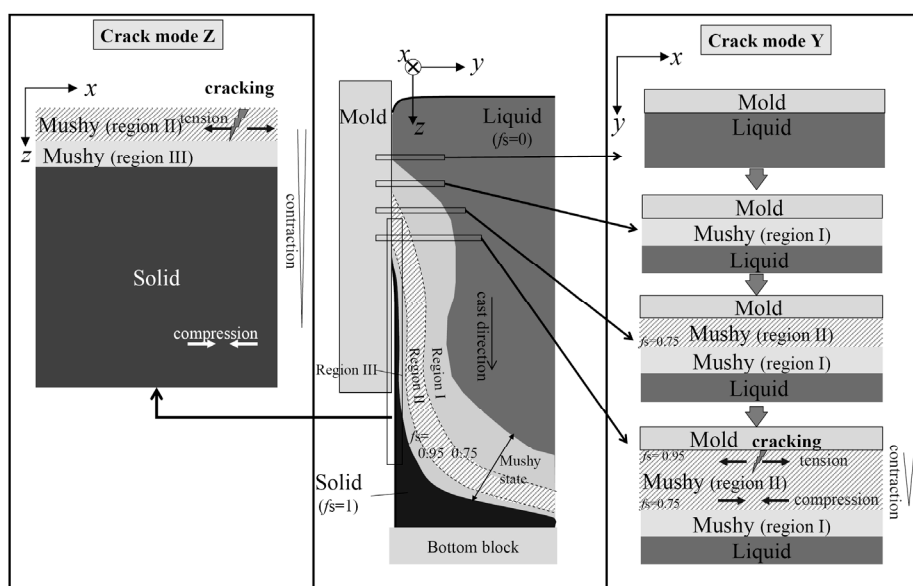


Fig. 3 Scheme of crack generation model.

(1) Crack mode due to a strain differences in the Z-direction (casting direction)

As shown in the “crack mode Z” of Fig.3, as to the vicinity of the surface of the ingot, the amount of shrinkage in x direction must be different between solid region and mushy region (Region II). Thus tensile strain should occur in the Region II. When the strain reaches the critical strain ϵ_c , crack occurs. This crack mode was designated as “crack mode Z” and it was assumed that the greater the absolute strain rate, the more easily cracked are ingots.

(2) Crack mode by the strain rate differences of the Y-direction (thickness direction)

As shown in “Crack mode Y” in Fig.3, the authors cited a crack mode caused by the difference of strain rates in the Y direction (thickness direction) of an ingot. The change in the temperature ΔT to the change in solid fraction Δf_s namely $\Delta T/\Delta f_s$ tend to be more negative with increase in solid fraction f_s , such as alloy g in Fig.4. With the assumption that $\Delta T/\Delta f_s$ is the same on Z direction at arbitrary moment, the shrink rate becomes larger, when the $\Delta T/\Delta f_s$ is more negative. The authors thought that the ingot is more susceptible to crack as the strain rate difference between the solid fraction of 0.75 and 0.95 at arbitrary moment. This crack mode was designated as “Crack mode Y.”

4.2.1 Estimation method of strain ε in “Crack mode Z” and crack index

In “Crack mode Z,” no crack occurs when the strain of the solid phase in the Region II of the surface layer is small. Because strain at the time of solidification occurs due to shrinkage of the solid phase, the amount of strain $\Delta l/l_0$ can be expressed by Eq. 1:

$$\Delta l/l_0 = \alpha \cdot \Delta T \quad (1)$$

where, l , α , and T denote length (m) in which shrinkage occurs, linear expansion coefficient (1/K), and temperature (K) of the portion, respectively, and the suffix 0 indicates the time before shrinkage occurs. The linear expansion coefficient can be expressed by Eq. 2:

$$\alpha = \alpha_s f_s + \alpha_L (1 - f_s) + \alpha_{SS} \quad (2)$$

Suffixes S, L and SS indicate the solid phase, liquid phase and just solidified phase, respectively. The first term and the second term on the right-hand side of Eq. 2 indicate the linear expansion coefficients of the solid phase and the liquid phase, respectively. And third term means linear expansion about solidification shrinkage. With respect to the solid phase portion in which dendrites form the skeleton, the solid phase shrinks in accordance with the linear expansion coefficient of the solid. On the other hand, since the liquid phase and solidified phase shrinks in a clearance of a skeletal structure formed in the solid phase in Region II, it was assumed that the liquid-phase and solidification shrinkage depended on the solid-phase shrinkage, that is, shrinkage of the skeletal portion. According to this assumption, α_L becomes equivalent to α_s , and the linear expansion coefficient can be expressed by Eq. 3:

$$\alpha \approx \alpha_s \quad (3)$$

Consequently, the strain rate $[\Delta l/l_0]_{II}$ of the Region II expressed by Eq. 3 can be expressed by Eq. 4 and is able to be compared with the critical strain ε_c .

$$[\Delta l/l_0]_{II} = \alpha_s \cdot \Delta T_{II} \quad (4)$$

ΔT_{II} denotes a difference between temperatures (T_1 and T_2 , respectively) at solid fractions 0.75 and 0.95 and can be estimated by Thermo-Calc (Fig. 5), and therefore, it was designated as one of the quantitative indexes that indicate crack sensitivity. It was assumed that crack is less likely to occur as ΔT_{II} (hereinafter referred to as the “brittle temperature range”) decreases.

4.2.2 Estimation method of strain ε in “Crack mode Y” and crack index

In this part of the section, it was investigated to express the strain rate in the Region II by formulation. With reference to Eq.(4) in the preceding section 4.2.1, the local strain is expressed by Eq. 5:

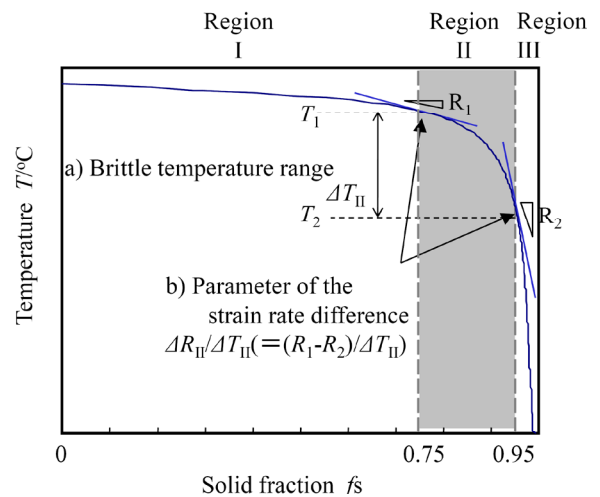


Fig. 4 Temperature-solid fraction curve calculated of “alloy g” and crack sensitivity indexes calculated by relation between solid fraction and temperature.

a) Brittle temperature range, ΔT_{II} .

b) Parameter of the strain rate difference, $\Delta R_{II}/\Delta T_{II}$.

$$\alpha_s = \frac{1}{l} \frac{\partial l}{\partial T} = \frac{\partial \ln l}{\partial T} \quad \text{from (both sides) } \times \partial T, \quad \partial \ln l = \alpha_s \partial T \quad (5)$$

In addition, because the solidification shell generated particularly in the vicinity of the surface is about 10 mm thick, it is assumed that the heat transfer from the liquid phase to the solid phase is rectilinear and there is no difference in heat fluxes that advance in the thickness direction. Consequently, if heat fluxes advance in the ingot thickness direction, that is, on the line in the heat flow direction, the same heat balance is obtained even if the location differs. The heat fluxes can be expressed by temperature changes of the solid phase and the liquid phase as well as the latent heat by phase changes and can be given by Eq. 6 [5].

$$q = \frac{m \overline{C_p}}{A} \frac{\partial T}{\partial t} + \frac{mL}{A} \frac{\partial f_s}{\partial t} = \text{const.} \quad (6)$$

where, q denotes heat fluxes (W/m^2), $\overline{C_p}$ and L average specific heat (J/kgK) and solidification latent heat (J/kg) of the solid and liquid phases, and m , A , and t the mass (kg), heat transfer cross-sectional area (m^2), and time (s). Eq. 6 can be expanded to the following equation:

$$\partial t = \frac{m}{qA} (\overline{C_p} \cdot \partial T + L \cdot \partial f_s) \quad (7)$$

By dividing Eq. 7 by Eq. 5, we have

$$\frac{\partial t}{\partial \ln l} = \frac{m}{\alpha_s \cdot qA} \left(\overline{C_p} + L \frac{\partial f_s}{\partial T} \right) \quad (8)$$

The left-hand side is a reciprocal of the strain rate, and this can be expressed by a reciprocal of the temperature change to the unit change in solid fraction (hereinafter $\partial T/\partial f_s$ is called “temperature gradient to solid fraction”).

α_s and $\overline{C_p}$ on the right-hand side is the value which is not greatly varied by alloys or temperatures. Therefore, the left-hand side of Eq. 8 increases as $\partial T/\partial f_s$ increases and can be expressed as follows:

$$\frac{\partial \ln l}{\partial t} \propto \frac{\alpha_s \cdot qA}{mL} \left(\frac{\partial T}{\partial f_s} \right) \quad (9)$$

Since $\partial T/\partial f_s$ can be estimated from the computations of Thermo-calc, using Eq. 9, the value of $\partial \ln l/\partial t$ equivalent to the strain rate can be obtained.

As shown in Fig. 4, at solid fractions of 0.75 and 0.95, which are both ends of the Region II, a difference of temperature gradient is most prominently generated in the strain rate.

$$R_1 \equiv \left[\frac{\partial T}{\partial f_s} \right]_{f_s=0.75}, R_2 \equiv \left[\frac{\partial T}{\partial f_s} \right]_{f_s=0.95} \quad (10)$$

As shown in Eq. 10, by setting $R_1(\text{K})$ and $R_2(\text{K})$, R_1-R_2 can be obtained as the quantitative value of the strain rate difference of the target alloy, and by designating this as a typical value, the strain rate difference that exerts effect on crack can be expressed. However, even if R_1-R_2 is large, the portions of solid fractions 0.75 and 0.95 are separated distantly, the distance from the restraint points is separated, and crack sensitivity lowers. In this way, the distance Δy of both solid fractions can be assumed to be proportional to the temperature difference between the solid fractions 0.75 and 0.95 ($T_1-T_2=\Delta T_{II}$), $\Delta y \propto \Delta T_{II}$, and the crack sensitivity can be expressed by Eq. 11:

$$\frac{R_1 - R_2}{\Delta y} \propto \frac{R_1 - R_2}{\Delta T_{II}} = \Delta R_{II} / \Delta T_{II} \quad (11)$$

Consequently, from Eq. 11, it was assumed that $(R_1-R_2)/\Delta T_{II}$ increased, crack sensitivity increased. Based on this, $(R_1-R_2)/\Delta T_{II}$ is used as another index to show the crack sensitivity and hereinafter it is called the parameter of the strain rate difference.

4.2.3 Verification of crack assessment results

Fig. 5 plots computed values of both indexes based on the alloying components submitted to experiments with the brittle temperature range ΔT_{II} and the parameter of strain rate difference $\Delta R_{II}/\Delta T_{II}$ used as coordinate axes. In addition, the casting rates at which crack occurs are shown by \odot \circ \triangle \times in order of difficulty to crack. The L-letter boundary line in the figure is the cracking boundary by casting rates (60, 80 and 100 mm/min).

This indicates that alloys with large values in both ΔT_{II} and $\Delta R_{II}/\Delta T_{II}$ generate crack even in low-speed casting, and in low-speed casting, the no-cracking region increases. Consequently, as a method for identifying the DC cast crack sensitivity, it is clarified that the method is effective technique to assess the crack sensitivity by the use of both indexes of ΔT_{II} and $\Delta R_{II}/\Delta T_{II}$.

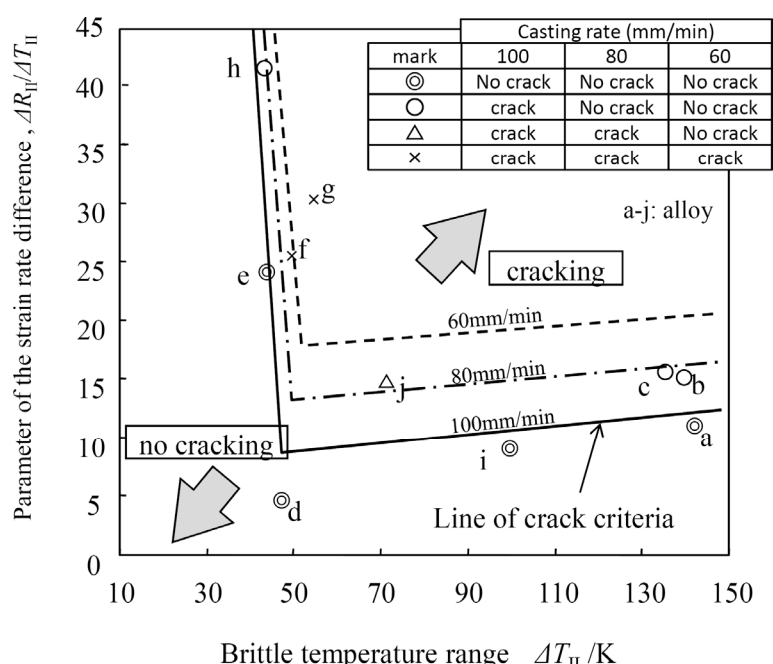


Fig. 5 Crack sensitivity assessment of each alloy by crack sensitivity indexes

5. Conclusion

Effects of alloying elements on surface cracks generated in aluminum DC casting had not always been accurately estimated, and therefore, efforts were made to develop a versatile and simple crack sensitivity assessment model as follows:

- 1) The region in which no melt was replenished even when the solid phase fractured was set to the solid fraction from 0.75 to 0.95, and it was surmised that crack occurred due to differences of strains and strain rates in this solid-fraction region (Region II).
- 2) It has been identified through experiments that a method for assessing DC cast crack sensitivity by the use of both indexes of the brittle temperature range ΔT_{II} and the parameter of strain rate difference $\Delta R_{II}/\Delta T_{II}$ is effective as a method for determining the cast crack sensitivity in DC casting.

References

- [1] H. Nagaumi, P. Suvanchai, T. Okane, T. Umeda: *Mat. Trans.*, Vol.47, No.12(2006), 2918-2924.
- [2] J. M. Drezet and M. Rappaz.: *Metall. Trans. A*, 30A(1999), 449-455.
- [3] H. Mizukami, Y. Shirai and A. Yamanaka: *ISIJ International*, **46**(2006), 1040-1046.
- [4] H. Mizukami, S Hiraki, M. Kawamoto and T. Watanabe: *Tetsu-to-Hagané*: **84**(1998), 763-769.
- [5] W. Kruz and D. J. Fisher: "Fundamentals of Solidification Fourth Revised Edition", (1998), 6.